J. Phys. B: At. Mol. Opt. Phys. 25 (1992) 5179-5197. Printed in the UK

Elastic and inelastic electron scattering by sodium at 10, 20 and 54.4 eV

B Marinković, V Pejčev, D Filipović, I Čadež and L Vušković†

Institute of Physics, 11001 Belgrade, PO Box 57, Yugoslavia

Received 16 March 1992, in final form 28 July 1992

Abstract. Relative differential electron impact cross sections ($\sigma(\theta)$) for elastic and inelastic (3p, 4s, 3d, 4p) scattering at 10 eV, 20 eV (3p and 4s excitation only) and 54.4 eV by sodium atom have been measured. The $\sigma(\theta)$ for the 3s–3p transition are normalized to the optical oscillator strength. The angular range of measurements is from 2° for inelastic and from 6° for elastic scattering, up to 150° for both. Results are compared with the available experimental and theoretical data. Present results of $\sigma(\theta)$ are lower at large scattering angles than coupled-channel theory predicts. Comparison with the recent distorted wave calculations by Madison *et al* is given in the following paper.

1. Introduction

Electron scattering by sodium at intermediate impact energies has been extensively studied over the past decade. Extensive research is put on reaching the 'complete' scattering experiment and determining magnitudes and phases of the scattering amplitudes. However, differential cross sections $\sigma(\theta)$ have not been known with satisfying accuracy.

Earlier experimental and theoretical works on electron–sodium collision cross sections have been summarized in a review paper by Bransden and McDowell (1978). In addition, $\sigma(\theta)$ for electron impact by sodium atom at 10, 20 and 54.4 eV electron impact energies have been measured by Gehenn and Reichert (1972, elastic), Shuttleworth *et al* (1977, 3p), Teubner *et al* (1978, elastic), Buckman and Teubner (1979, 3p), Srivastava and Vušković (1980, elastic, 3p, 4s, 3d+4p, 4d+4f+5p+5s), Teubner *et al* (1986, 3p), Allen *et al* (1987, elastic), Lorentz and Miller (1989, elastic and 3p) and Jiang *et al* (1990, 3p). Calculations of $\sigma(\theta)$ have been done by Hertel and Rost (1971, second Born approximation: 4s), Carse (1972, two-state close coupling (CC2): elastic and 3p), Walters (1973, Glauber approximation: elastic and 3p), Kennedy *et al* (1977, distorted-wave polarized-orbital (DWPO): 3p), Issa (1977, impact parameter and CC2 with second order potential: elastic and 3p), Teubner *et al* (1978, optical model: elastic), McCarthy *et al* (1985, coupled-channel optical (CCO) theory: elastic, 3p, 4s and 3d), Mitroy *et al* (1987, CCO: elastic, 3p, 4s and 3d), Oza (1988, CC4: elastic), Gien (1988, modified Glauber approximation: elastic), Msezane *et al* (1988, CC2, CC3,

† Present address: New York University, Physics Department, New York, NY 10003, USA.

CC4 and CC6: 4s), Balashov *et al* (1989, distorted-wave with a phenomenological optical potential: elastic, 3p), Bray *et al* (1991a, 3CCO: elastic and 3p), Bray *et al* (1991b, 1CCO: elastic) and most recently by Madison *et al* (1992, second-order distorted wave including exchange: elastic, 3p, 4s and 4p).

The need for new measurements was stressed by Mitroy *et al* (1987) since large discrepancies exist between theory and experiment as well as among the experiments themselves. Their close coupling calculations give large angle $\sigma(\theta)$ higher than any experiment. Msezane *et al* (1988) investigated the problem of converging the cross sections upon the number of states used in CC calculations.

In this paper we present relative differential cross sections at 10 eV (elastic, 3p, 4s, 3d and 4p), 20 eV (elastic, 3p and 4s) and 54.4 eV (elastic, 3p, 4s, 3d and 4p) electron impact energies. The angular range is from 2° for inelastic and from 6° for elastic scattering, both up to 150°. By normalization to the optical oscillator strength for the 3s–3p transition, the 3^2P $\sigma(\theta)$ were put on an absolute scale. The ratios of the other measured $\sigma(\theta)$ and resonant (3^2P) cross sections at a particular angle are obtained by comparing relative heights of the peaks in energy loss spectra. Integral cross sections are determined from the differential ones. Preliminary results on these measurements have been reported at conferences (Marinković *et al* 1988, 1989).

2. The experiment

The electron impact spectrometer used for the present measurements has been described elsewhere (Filipović *et al* 1988). It consists of an electrostatic hemispherical energy selector and cylindrical lenses in the monochromator as well as in the analyser. The spheres are baked and both selector and analyser are differentially pumped relative to the main chamber. The double μ-metal shields were used to reduce the magnetic field to below 0.1 μT. The overall energy resolution was about 50 meV so that 3^2D and 4^2P peaks, separated by approximately 140 meV, were well resolved in the energy-loss spectrum (see figure 1). The energy scale was determined by the threshold energy for the 3p excitation and may be in error up to 0.2 eV.

An atomic Na beam was generated from a stainless steel crucible containing sodium sample heated by coaxial wire (Marinković 1988). The Na beam was perpendicularly crossed by an energy-selected electron beam.

The angular intensity distribution of the 3p excitation was measured at two oven temperatures. A reduced oven temperature of 500 K was used in the angular range from 2° to 20° in order to avoid saturation problems of the channeltron detector due to a very intense signal. A temperature of 600 K was high enough to allow good statistics in a deep minimum and it has been used to obtain the angular distribution from 10° to 150°. The nozzle was maintained at a temperature 50 K higher than the crucible. Before each measurement the energy-loss spectrum was taken to verify the absence of double scattering. The background count rate never exceeded 5% of the scattering signal and it was subtracted from the measured intensity. The background pressure was 5×10^{-5} Pa.

The scattering intensity distribution as a function of the scattering angle was measured by adjusting the detector to record only those electrons with an energy loss corresponding to a particular transition. The zero scattering angle was determined by the symmetry of the 3p angular distribution from −20° to +20°. It was possible to achieve a mechanical precision of 0.2° in the angular positioning of the analyser.

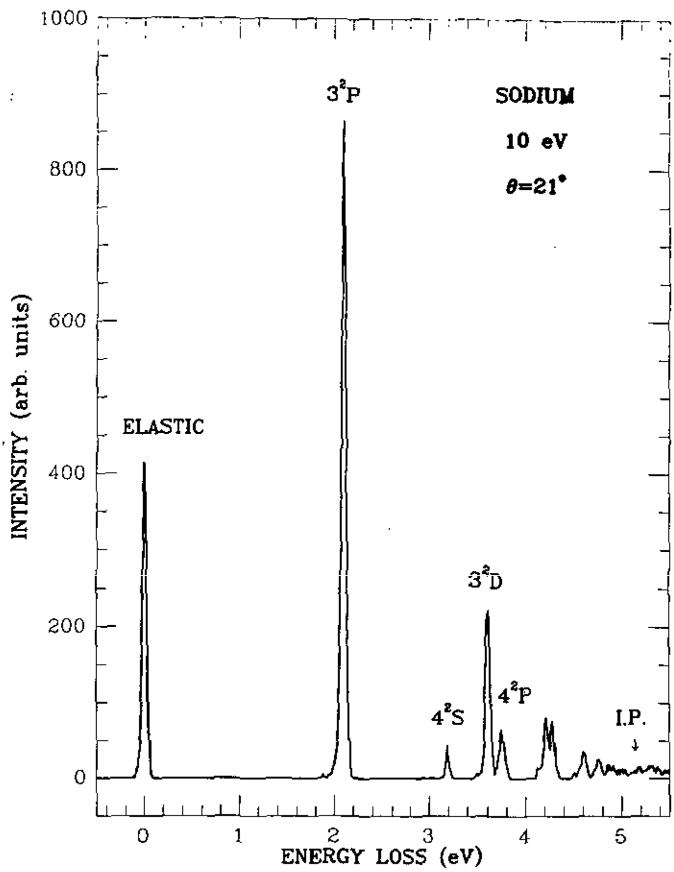

Figure 1. Energy loss spectrum of the sodium atom at 10 eV electron impact energy and 21° scattering angle.

To estimate the angular resolution of our experiment we have considered: (i) the acceptance angle of the analyser, (ii) the shape of atomic beam and (iii) the spatial electron beam distributions.

(i) The acceptance angle is defined by two coaxial circular apertures in the field free entrance region of the analyser. The diameters of the apertures are 0.4 and 0.7 mm and the distance between them is 12 mm. This gives an acceptance angle of 2.6°. The full width of the detecting cone at the plane of interaction region is then 2.4 mm.

(ii) If the atomic beam is completely viewed by the analyser acceptance angle, it does not influence the angular resolution. This was proven since no influence was noticed by changing the distance of the nozzle from the interaction region (1.5, 2 and 3 mm), i.e. choosing different sizes of the atomic beam. A low pressure in the oven (less than 10 Pa) and an 8 mm long nozzle with a 1.4 mm inner diameter provide an effusive atomic beam.

(iii) The spatial distribution of the electron beam at different impact energies was measured. The width of the electron beam at the plane of the interaction volume was found to be 0.9 mm at energies 54.4 and 20 eV, and 1.1 mm at energy 10 eV. These widths were determined from the angular spread of the electron beam (1.1° and 1.5°, respectively).

Experimental determination of the angular resolution could be done by measuring the depth of narrow minima in $\sigma(\theta)$. The obtained depth would reflect the angular resolution of the apparatus. Such minima in $\sigma(\theta)$ for sodium atom do not exist in the energy interval studied. From the above considerations (i)–(iii) the angular resolution in the present measurements is estimated to be 1.5°.

The angular dependences of the scattering signal were corrected for an effective path length to get relative $\sigma(\theta)$. The effective path length corrections were estimated for sodium as a target, the present scattering geometry and the beam densities using the method of Brinkmann and Trajmar (1981).

The absolute $\sigma(\theta)$ for the 3p excitation was obtained by normalization to the optical oscillator strength, $f^\circ = 0.982$ (Wiese *et al* 1969). The generalized oscillator strength (GOS) defined in atomic units as

$$f_{0n}^{G} = \tfrac{1}{2} W (k_0/k_n) K^2 \sigma(\theta)$$

where W is the excitation energy, k_0 and k_n are initial and final electron momenta, respectively, and K is the momentum transfer, is plotted as a function of K^2. An example of GOS for 10 eV is shown in figure 2. The experimental points were fitted to

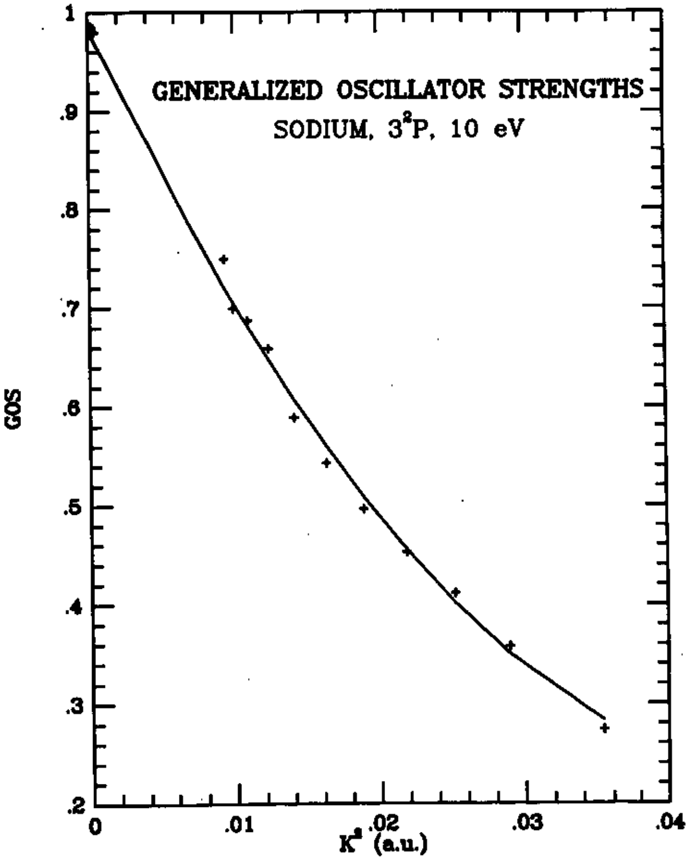

Figure 2. Generalized oscillator strengths at 10 eV plotted against squared momentum transfer: ●, optical oscillator strength ($f^\circ = 0.982$); +, present; ——, fit of experimental data normalized to f°.

the curve (Vušković *et al* 1982)

$$f_{0n}^{G} = f^{o} + aK^2 + bK^4$$

where a and b are fitting coefficients.

3. Results and discussion

This experiment was performed with electron impact energies of 10, 20 and 54.4 eV. The intensity distributions were measured for elastic scattering and the excitation of the 3^2P and 4^2S states at all three energies. The 3^2D and 4^2P states were studied at 10 and 54.4 eV only. The elastic scattered electron intensities were recorded from 10° to 150° in the steps of 10°. The scattering intensities for the resonant transition 3^2P were recorded at every 2° in the range of small scattering angles because this range is particularly relevant for the normalization procedure.

Measured $\sigma(\theta)$ are presented in tables 1 to 5 and figures 3 and 5 to 9. Intensity ratios between the 3^2P excitation and elastic or other inelastic peaks were determined by obtaining several energy loss spectra at different scattering angles. As all peaks are only 2 eV apart one from another we did not take into account the analyser transmission. That is the reason why we present our results in relative units except for $\sigma(\theta)$ for the 3^2P state. Measured intensity ratios are given in table 6 from which tentative absolute values for elastic and other inelastic transitions could be obtained.

Results for the 3^2P state are presented in table 1 and figure 3. At higher impact energies the $\sigma(\theta)$ are strongly forward peaked and span seven orders of magnitude. There are two minima in $\sigma(\theta)$ which become shifted to smaller scattering angles with increasing impact energy and the second one becomes deeper. As stated above, the $\sigma(\theta)$ are put on an absolute scale by normalization to the optical oscillator strength. Generalized oscillator strengths (GOS) obtained by different authors at 54.4 eV are presented in figure 4. Our measured points are extrapolated to $f^{o} = 0.982$. The slope of the GOS curve is steeper than predicted by close coupling theories but it is the same as the DWPO theory by Kennedy *et al* (1977). Measurements by Buckman and Teubner (1979) and Shuttleworth *et al* (1977) also have steeper slopes but their values at zero squared momentum transfer exceed the value of 0.982. The measurements of Lorentz and Miller (1989) follow the predictions of close coupling theories. These measurements were normalized onto integral cross sections obtained by the same theoretical calculations. For comparison with other authors the $\sigma(\theta)$ at 10 eV are chosen and presented in figure 5. Our results are in fair agreement at smaller scattering angles but at larger ones, the $\sigma(\theta)$ are lower. It is interesting that the present $\sigma(\theta)$ show a second minimum at 130° while CC4 theory (Mitroy *et al* 1987) predicts it at 160° or 3CCO theory (Bray *et al* 1991a) gives no second minimum. Again DWPO (Kennedy *et al* 1977) theory shows a better agreement with the present experiment. $\sigma(\theta)$ at 20 eV are in agreement with the measurements of Srivastava and Vušković (1980) and with the CCO theories of Mitroy *et al* (1987) and Bray *et al* (1991a). Measurements made by Teubner *et al* (1986, at 22.1 eV) and Lorentz and Miller (1989, at 20 eV) are smaller by a factor of 2.5 at 90° scattering angle. The $\sigma(\theta)$ at 54.4 eV is strongly forward peaked and it has two minima at 50° and 110°. The present data agree well with the previous measurements by Srivastava and Vušković (1980) in the medium range of scattering angles. This agreement is important because the two experiments utilized different normalization procedures. But the present data are higher by 20% to 30% at smaller scattering angles

Table 1. Differential cross sections for excitation of the 3^2P state of sodium in units of 10^{-20} m^2 sr^{-1}. The values in parentheses are absolute errors. The last three lines are the calculated integral (Q_I), momentum transfer (Q_M), and viscosity (Q_V) cross sections with their respective absolute errors in units of 10^{-20} m^2.

θ (deg)	10 eV	20 eV	54.4 eV
0			
2	454 (68) E−0		104 (14) E+1
4	345 (51) E−0		265 (36) E−0
6	215 (32) E−0	273 (40) E−0	883 (121) E−1
8	134 (20) E−0		366 (53) E−1
10	795 (117) E−1	798 (123) E−1	158 (22) E−1
15			187 (27) E−2
20	532 (170) E−2	505 (61) E−2	357 (48) E−3
30	745 (221) E−3	588 (140) E−3	563 (74) E−4
40	316 (68) E−3	315 (49) E−3	156 (24) E−4
50	138 (34) E−3	760 (163) E−4	978 (165) E−5
60	556 (140) E−4	463 (77) E−4	108 (15) E−4
70	171 (51) E−4	545 (98) E−4	100 (13) E−4
80	142 (55) E−4	878 (142) E−4	769 (124) E−5
90	359 (153) E−4	852 (127) E−4	408 (65) E−5
100	310 (74) E−4	644 (89) E−4	130 (24) E−5
110	456 (84) E−4	389 (65) E−4	736 (164) E−6
120	213 (34) E−4	179 (32) E−4	345 (54) E−5
130	163 (31) E−4	322 (41) E−4	116 (23) E−4
140	228 (53) E−4	425 (76) E−4	288 (57) E−4
150	341 (70) E−4	907 (154) E−4	515 (103) E−4
Q_I	294 (48) E−1	356 (70) E−1	198 (30) E−1
Q_M	411 (69) E−2	307 (56) E−2	694 (108) E−3
Q_V	724 (120) E−2	495 (87) E−2	976 (143) E−2

and at larger scattering angles they are lower by approximately 50%. The experimental results of Buckman and Teubner (1979) are generally lower by a factor of three compared to our results. This is because their angular distribution is more forward peaked than ours and this influences the normalization to f°. The reason for that may be because of better angular resolution (they claim 0.5°) or because of the presence of double scattering in their experiment. The results of theoretical calculations by McCarthy *et al* (1985), Mitroy *et al* (1987) and Bray *et al* (1991a) are higher than ours at 30° by factors of 1.4, 1.5 and 1.1, at 100° by factors 4.5, 6.4 and 3.4 and at 150° by factors 2.3, 1.9 and 1.7, respectively. This discrepancy probably results from partial-wave convergence as was noticed by Msezane (1988) and Msezane *et al* (1988) who utilized CC2, CC4 and CC6 calculations. But the same theory accurately predicted the angular behaviour of unpolarized angular momentum transfer perpendicular to the scattering plane, $L_\perp$, as was proven in experiments by McClelland *et al* (1989). However, the parameter $L_\perp$ seems rather insensitive to the theory used (Kelley 1990).

Results for the elastic scattering are presented in table 2 and figure 6. The angular dependences of elastic scattering were measured separately. At 10 eV there are two minima in $\sigma(\theta)$, the first being prominent. With increasing impact energy the second one becomes exceedingly dominant. The shape of $\sigma(\theta)$ at 10 eV is the same as in other experiments (Gehenn and Reichert 1972, Srivastava and Vušković 1980) and theoretical calculations (Mitroy *et al* 1987, Oza 1988, Bray *et al* 1991a) except that the second

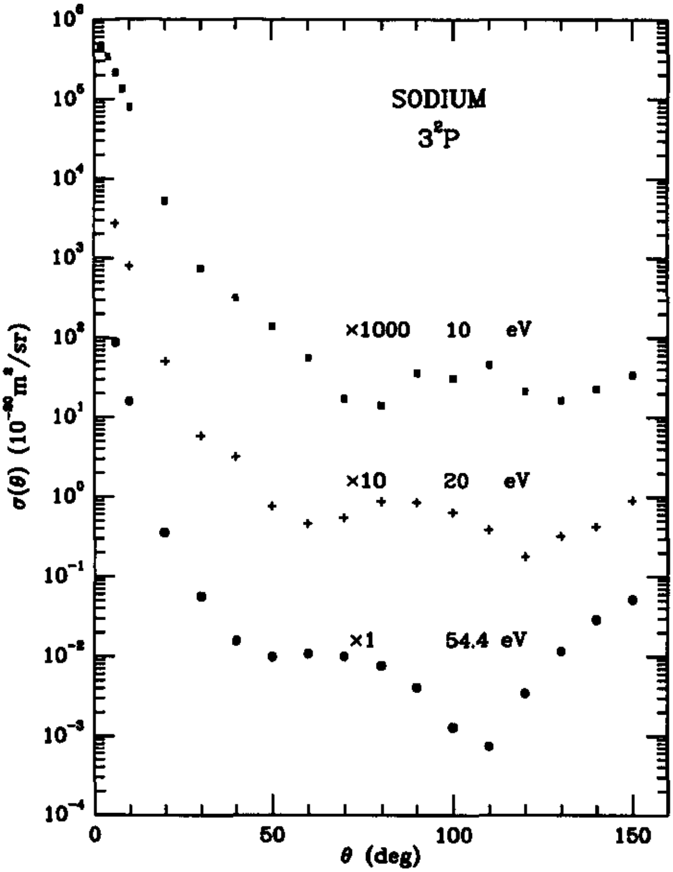

Figure 3. Differential cross sections for 3^2P at 10, 20 and 54.4 eV are normalized to the optical oscillator strength. The $\sigma(\theta)$ at 20 eV are multiplied by 10 and at 10 eV by 1000 for a clear presentation.

minimum at the present experiment is at 140° while theories give 150°. The $\sigma(\theta)$ at 20 eV are in good agreement with the data of Lorentz and Miller (1989). The measured points around the first minimum at 45° are not closely spaced in the present experiment while the second minimum is more pronounced than in Lorentz and Miller experiment. The $\sigma(\theta)$ at 54.4 eV, obtained from 6° to 150°, have one minimum at 110°. The minimum at 110° is not so sharp as it is in the Teubner *et al* (1978) data, but it is deeper than in the measurements by Srivastava and Vušković (1980).

Results for the 4^2S state are presented in table 3 and figure 7. The shapes of $\sigma(\theta)$ closely resemble those of elastic scattering since this state is of the same symmetry as the ground state. $\sigma(\theta)$ at 10 eV has the same slope as the calculations by Mitroy *et al* (1987). The second minimum is found at 140° while the theory predicts 160°. The slope of experimental values by Srivastava and Vušković (1980) is different to ours at small scattering angles. The $\sigma(\theta)$ at 20 eV are almost the same as those of Srivastava and Vušković (1980) in the angular range from 20° to 120°, the largest scattering angle obtained in previous experiment. At angles smaller than 60° our $\sigma(\theta)$ follow calculations by Mitroy *et al* (1987) while for the larger angles they are smaller than theory predicts. The $\sigma(\theta)$ at 54.4 eV are in agreement with the measurements of Srivastava and Vušković

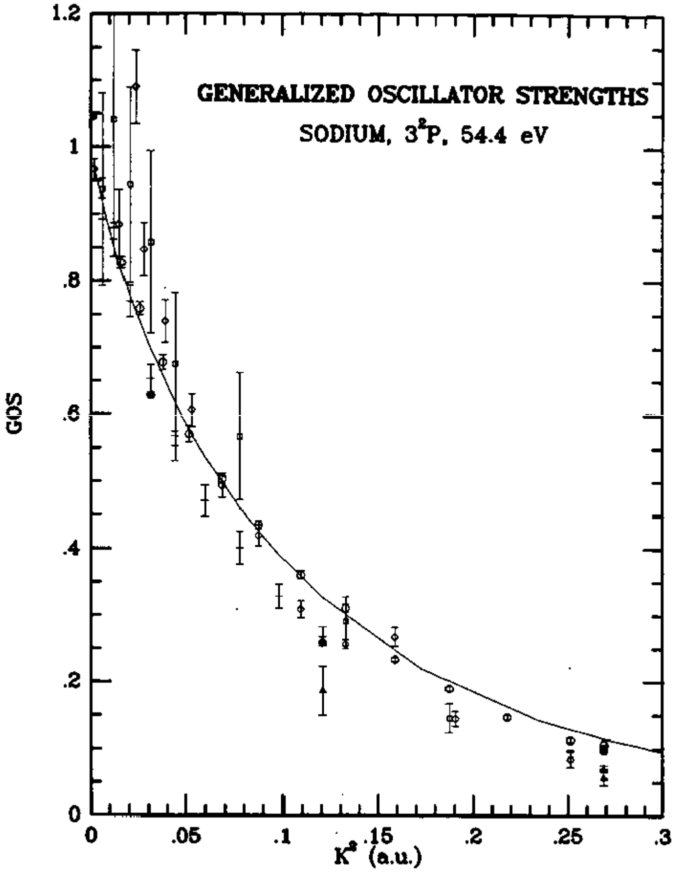

Figure 4. Generalized oscillator strengths at 54.4 eV plotted against squared momentum transfer: +, present; ●, Kennedy *et al* (1977); ——, Mitroy *et al* (1987); ◇, Shuttleworth *et al* (1977); ⊡, Buckman and Teubner (1979); △, Srivastava and Vušković (1980); ○, Lorentz and Miller (1989).

(1980) and calculations of Msezane *et al* (1988) in the angular range from 10° to 140°. For angles smaller than 10°, the $\sigma(\theta)$ agree with the second Born calculations of Hertel and Rost (1971).

Results for the 3^2D and 4^2P states are presented in tables 4 and 5 and figures 8 and 9, respectively. While $\sigma(\theta)$ for the 4^2P resembles the shape of the 3^2P state, $\sigma(\theta)$ for the 3^2D state is rather flat at larger scattering angles. At small scattering angles the 3^2D peak is stronger than the 4^2P peak in energy loss spectra. The energy resolution in the experiment of Srivastava and Vušković (1980) was not sufficient to resolve these states.

Integrated cross sections (integral, momentum transfer and viscosity cross sections defined as in Marinković *et al* 1991) were obtained by extrapolating $\sigma(\theta)$ to 0° and 180° scattering angles and integrating over solid angle. Extrapolation to 0° was made by using the fitting curve for generalized oscillator strength for the 3^2P excitation. The theoretical data of Mitroy *et al* (1987) were used as a guide for the shape of elastic $\sigma(\theta)$. The same theory was utilized for high angle scattering up to 180° in both cases.

Statistical errors which account for signal intensity and averaging over different sets of measurements are determined for every $\sigma(\theta)$ at each scattering angle. At low

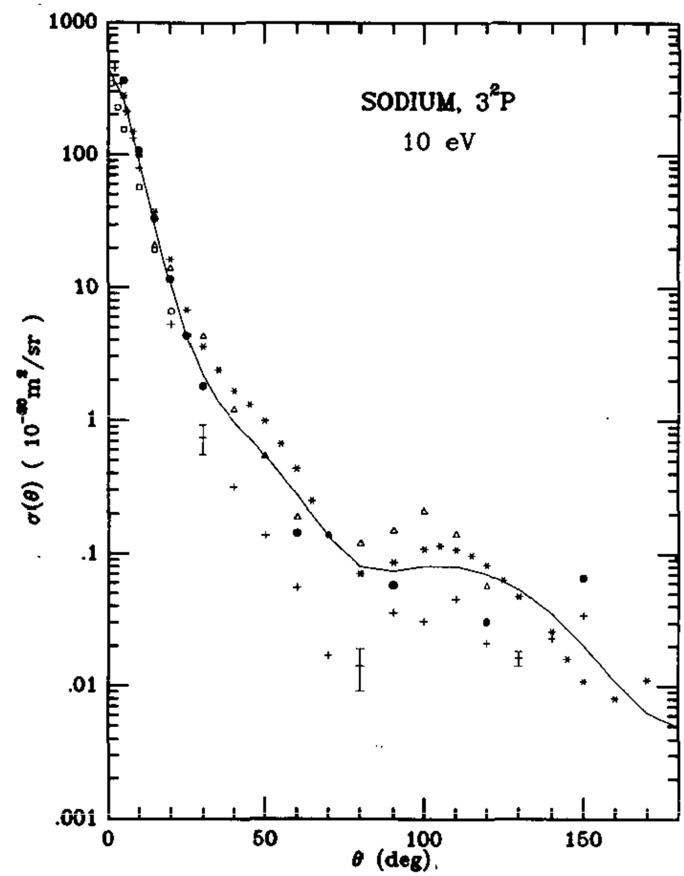

Figure 5. Differential cross sections for 3^2P at 10 eV: +, present (statistical error indicated); ●, Kennedy *et al* (1977); *, Mitroy *et al* (1987); ——, Bray *et al* (1991a); △, Srivastava and Vušković (1980); □, Jiang *et al* (1990).

scattering angles (up to 20°) they were on average 8.6% for elastic, 6.3% for the 3^2P $\sigma(\theta)$ and 9.9% for the other inelastic $\sigma(\theta)$. The averaged statistical error at the minima reached 15%, 15% and 33%, respectively. Contributions to the error of the cross section value which is due to the uncertainty of the energy scale is largest at 10 eV and is estimated to be 0.5%, 0.2% and 0.5% for the elastic, the 3^2P and the other inelastic $\sigma(\theta)$, respectively. Contributions to this error due to the uncertainty of the angular scale is the largest where $\sigma(\theta)$ is strongly forward peaked, i.e. at small scattering angles and large impact energies. At 54.4 eV it is estimated to be 4.3%, 8.7% and 5.7% for the elastic, the 3^2P and the other inelastic $\sigma(\theta)$, respectively. In order to estimate the effects of the angular variation of the electron-beam–atom-beam interaction region through the applied geometrical effective path length corrections we have examined several different correction functions. The whole normalization procedure was redone for each case. The observed deviations in cross section correspond to uncertainties of 8.9%, 2.2% and 7.9% at 10, 20 and 54.4 eV impact energies, respectively. The optical oscillator strength is known with 3% accuracy. The error associated with the fitting the extrapolation procedure to $f°$ is larger at small impact energies and it was estimated to be 9.8% (at 10 eV), 9.0% (20 eV) and 5.0% (54.4 eV). The total error for the absolute $\sigma(\theta)$ value

Table 2. Relative cross sections for elastic scattering of sodium normalized to unity at 90°. The values in parentheses are statistical errors in the intensity measurements. The last three lines are the calculated integral (Q_I), momentum transfer (Q_M), and viscosity (Q_V) cross sections in relative units. The values in parentheses are total errors for the integrated cross sections in the same relative units.

θ	10 eV	20 eV	54.4 eV
0			
6			131 (2) E+1
10		192 (4) E−0	525 (5) E−0
15	209 (6) E−0		165 (7) E−0
20	761 (314) E−1	266 (28) E−1	637 (26) E−1
30	678 (327) E−2	378 (35) E−2	159 (8) E−1
40	807 (305) E−3	732 (69) E−3	815 (35) E−2
50	192 (11) E−3	824 (76) E−3	511 (20) E−2
60	283 (77) E−3	130 (17) E−2	369 (17) E−2
70	661 (100) E−3	139 (8) E−2	322 (21) E−2
80	857 (215) E−3	126 (18) E−2	196 (13) E−2
90	100 (14) E−2	100 (8) E−2	100 (6) E−2
100	800 (91) E−3	584 (51) E−3	252 (21) E−3
110	693 (62) E−3	352 (38) E−3	851 (87) E−4
120	467 (52) E−3	176 (28) E−3	631 (40) E−3
130	233 (37) E−3	245 (33) E−3	214 (17) E−2
140	212 (42) E−3	703 (56) E−3	420 (41) E−2
146			631 (47) E−2
148		127 (9) E−2	685 (10) E−2
150	376 (46) E−3	138 (14) E−2	774 (16) E−2
Q_I	215 (52) E−0	868 (126) E−1	249 (39) E−0
Q_M	107 (25) E−1	124 (20) E−1	439 (69) E−1
Q_V	141 (36) E−1	961 (162) E−2	268 (42) E−1

for the 3^2P excitation indicated in table 1 is obtained for each point as the square root of the sum of squared errors: statistical error, uncertainty due to the energy scale, due to the angular scale, due to V_{eff}, due to f°, and due to fitting to f°. The error of the relative cross sections in tables 2-5 are only statistical ones. If the absolute values are to be obtained an adequate error of normalization should be added. If the normalization to the optical oscillator strength is to be used then for scattering processes other than the resonant one, the error in the determination of the intensity ratios (given in table 6) should be included.

For the integrated cross sections additional errors due to extrapolation to zero and 180° and the numerical integration procedure are considered. For the integral cross section the most critical is extrapolation for elastic scattering due to the fact that the major contribution comes from small scattering angles where measurements of the elastic signal are limited. This error is estimated to be on average 7.8% for elastic, 7.4% for the 3^2P and 4.9% for the other inelastic $\sigma(\theta)$. For the momentum transfer cross sections extrapolation to large scattering angles becomes relatively more important due to the $(1-\cos(\theta))$ term. The errors in this case are estimated to be on average 3.6% for elastic, 6.8% for the 3^2P and 2.3% for the other inelastic $\sigma(\theta)$. The errors for the viscosity cross sections for the same states due to extrapolation are estimated to be on average 0.5%, 5.8% and 0.4%, respectively. The contributions to the error due to numerical integration procedure are small and are on average 1.5% for the integral

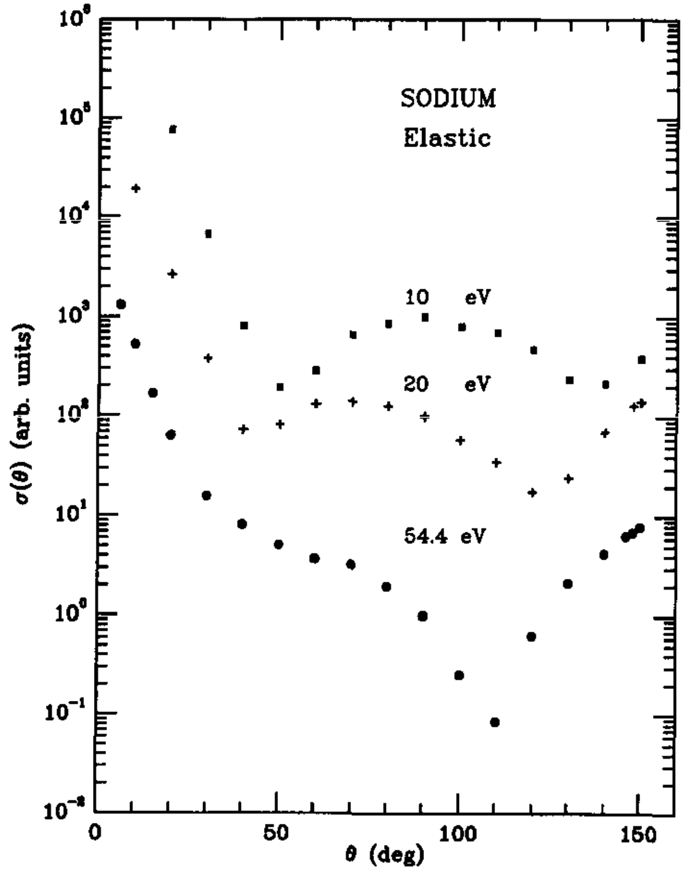

Figure 6. Relative differential cross sections of elastic scattering at 10, 20 and 54.4 eV.

cross sections, 0.9% for the momentum transfer and 1.4% for the viscosity cross sections. The absolute errors for integrated cross sections for the 3^2P are given in table 1. For the elastic and other inelastic integrated cross sections errors are indicated in tables 2–5.

The source of error in sodium experiments may be the double electron scattering to the resonant transition as cross sections are very large at small scattering angles. The double scattering can be observed as a peak at 4.204 eV in energy-loss spectra taken with high resolution since the energy losses of the nearby 5^2S and 4^2D peaks are at 4.116 eV and 4.284 eV, respectively. As we performed the experiment with 50 meV resolution we have systematically checked for the absence of the doubly scattering contributions.

The experimental intensity ratios for the $\sigma(\theta)$ for elastic and inelastic transitions at the particular scattering angle with respect to the value of the $\sigma(\theta)$ for the 3^2P state at the same angle are presented in table 6. These ratios were obtained by systematic analysis of the energy loss spectra under different focusing conditions in both exit selector and entrance analyser optics. Intensity ratios of elastic to the 3^2P excitation at 54.4 eV was determined to be 0.558 ± 0.015 at 10° and 5.4 ± 0.5 at 60° (statistical error indicated only). The errors indicated in table 6 are total errors in the intensity ratio measurements and they include statistical error and the errors due to uncertainties of the angular scale. As discussed previously, in order to obtain the absolute values for

Table 3. Relative cross sections for the 4^2S state normalized to unity at 90°. The values in parentheses are statistical errors in the intensity measurements. The last three lines are the calculated integral (Q_I), momentum transfer (Q_M), and viscosity (Q_V) cross sections in relative units. The values in parentheses are total errors for the integrated cross sections in the same relative units.

θ	10 eV	20 eV	54.4 eV
0			
2	679 (5) E−0	126 (15) E+1	147 (5) E+2
4	545 (4) E−0	866 (100) E−0	673 (22) E+1
6	384 (4) E−0	589 (77) E−0	314 (7) E+1
8		371 (42) E−0	150 (3) E+1
10	193 (3) E−0	222 (30) E−0	741 (39) E−0
15			928 (66) E−1
20	333 (11) E−1	182 (27) E−1	432 (41) E−1
30	110 (6) E−1	439 (54) E−2	244 (19) E−1
40	502 (44) E−2	171 (15) E−2	110 (11) E−1
50	219 (30) E−2	750 (28) E−3	649 (37) E−2
60	988 (154) E−3	848 (56) E−3	560 (71) E−2
70	501 (119) E−3	120 (2) E−2	315 (47) E−2
80	635 (129) E−3	114 (4) E−2	205 (58) E−2
90	100 (15) E−2	100 (5) E−2	100 (24) E−2
100	706 (134) E−3	689 (48) E−3	496 (24) E−3
110	112 (16) E−2	324 (24) E−3	651 (523) E−4
120	743 (138) E−3	138 (22) E−3	477 (224) E−3
130	323 (105) E−3	103 (30) E−3	178 (74) E−2
140	107 (79) E−3	213 (46) E−3	378 (104) E−2
148			665 (152) E−2
150	177 (90) E−3	625 (56) E−3	
Q_I	825 (160) E−1	871 (182) E−1	470 (83) E−0
Q_M	231 (48) E−1	156 (30) E−1	592 (120) E−1
Q_V	349 (69) E−1	216 (43) E−1	568 (108) E−1

the excitation of the 3^2P state normalization to the f° was used. This normalization, even without physical justification for lower energies, was used to estimate the absolute values based on an independent and accurate measurement of the f°. Also, one can explore the limits of the applicability of this method comparing results with those obtained with different normalization methods discussed in the next paragraph. The renormalization of the data presented in table 1 by some other method is simple and straightforward. Therefore, a physical insight on the limitations of the Born approximation is possible through such a comparison.

Normalization factors for $\sigma(\theta)$ for different normalization procedures are presented in table 7. The $\sigma(\theta)$ obtained by multiplying values given in tables 1–5 by these normalization factors are in units of $10^{-20}\,m^2\,sr^{-1}$ while the integrated cross sections are in units of $10^{-20}\,m^2$. Factors based on the normalization to the f° for the 3^2P state are listed in column A. For the 3^2P state factors are equal to unity while for the other $\sigma(\theta)$ they are obtained from the intensity ratio measurements presented in table 6. They immediately give absolute values of the $\sigma(\theta)$ at 90°. For an alternative normalization all the measured inelastic relative $\sigma(\theta)$ were extrapolated to zero and 180° angular range, integrated and then normalized to the optical excitation function measurements

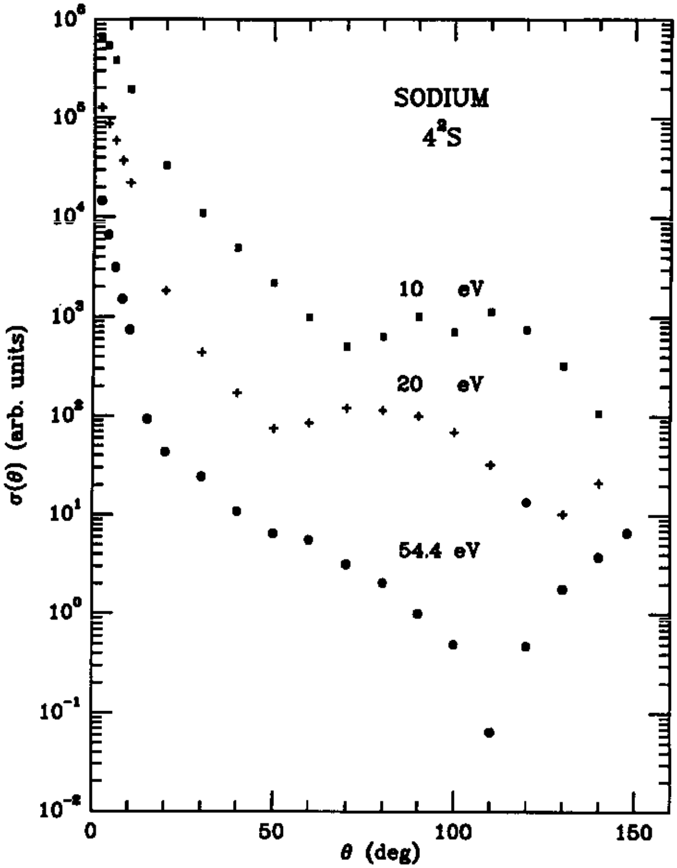

Figure 7. Relative differential cross sections of 4^2S at 10, 20 and 54.4 eV.

of Phelps and Lin (1981). These direct excitation functions are determined with the uncertainties of 12% for the 3^2P state, 15% for the 3^2D state and 40% for the 4^2S and 4^2P states. Cubic spline interpolation was used to obtain values for the energies not tabulated by these authors. The corresponding normalization factors are given in column B. Factors for the normalization to the theoretical results of non-relativistic second-order distorted wave (DWB2PE) theory with full treatment of polarization and exchange distortion by Madison *et al* (1992) are presented in column C. These factors are obtained by equating the partial integral cross section over the measured angular range to DWB2PE theory integrated over the same angular range. In this case error due to the extrapolation is eliminated.

Several conclusions can be drawn out from the integral cross sections (Q_I) calculated on the basis of the coefficients presented in table 7. At 10 eV the relative cross sections for the inelastic processes (relative to 3^2P) calculated from column A are in a very good agreement with the values normalized to the experimental results of Phelps and Lin (1981) (column B) but the latter are on average about 25% higher than the former ones. This good agreement indicates a constant scattered electron transmission and satisfactory extrapolation to zero and 180°. The lower values of our absolute cross sections are due to the inapplicability of the normalization to f° at this impact energy,

Table 4. Relative cross sections for the 3^2D state normalized to unity at 90°. The values in parentheses are statistical errors in the intensity measurements. The last three lines are the calculated integral (Q_I), momentum transfer (Q_M), and viscosity (Q_V) cross sections in relative units. The values in parentheses are total errors for the integrated cross sections in the same relative units.

θ	10 eV	54.4 eV
0		
2		135 (1) E+3
4		646 (24) E+2
6	132 (65) E+1	338 (11) E+2
8		205 (1) E+2
10	889 (179) E−0	121 (2) E+2
15		201 (2) E+1
20	196 (56) E−0	313 (8) E−0
30	415 (149) E−1	343 (9) E−1
40	138 (31) E−1	146 (14) E−1
50	623 (69) E−2	797 (86) E−2
60	285 (7) E−2	535 (34) E−2
70	131 (11) E−2	296 (41) E−2
80	959 (91) E−3	235 (24) E−2
90	100 (8) E−2	100 (19) E−2
100	898 (58) E−3	653 (176) E−3
110	109 (13) E−2	790 (208) E−3
120	634 (38) E−3	830 (125) E−3
130	415 (105) E−3	315 (21) E−2
140	334 (104) E−3	502 (56) E−2
146		908 (162) E−2
150	371 (97) E−3	
Q_I	318 (88) E−0	480 (83) E+1
Q_M	837 (228) E−1	282 (53) E−0
Q_V	138 (38) E−0	428 (75) E−0

which is only about five times the excitation energy. The results at 10 eV obtained by the normalization to the theoretical cross sections of Madison *et al* (1992) (column C) are significantly different from the experimental ones by the absolute values as well as by the relative intensities. We believe that the disagreement in the elastic cross sections can partially be attributed to the lower electron transmission for elastically scattered electrons in our experiment at the lowest electron energy. For the 3^2P state the data normalized to this theory are approximately 36% higher than ours but the others are higher by about two times (4^2S) to 16 times (4^2P). Strong disagreement also exists for 4^2P state at 54.4 eV. We do not believe that it can be due to the transmission variation in our experiment. Namely, 3^2D and 4^2P peaks lie close enough in energy-loss spectra and this variation should be small. The comparison with the data of Phelps and Lin gives us additional confidence that our relative intensities are correct. The integral cross sections for the 3^2P state at 20 eV and 54.4 eV for all three methods of normalization agree within ±10% which can be considered satisfactory. This indicates that the $\sigma(\theta)$ can be normalized to f° for energies above about 20 eV (10 times excitation energy). There is satisfactory agreement in the relative Q_I obtained with all three methods for the 4^2S state at both energies 20 eV and 54.4 eV. The agreement of the

Table 5. Relative cross sections for the 4^2P state normalized to unity at 90°. The values in parentheses are statistical errors in the intensity measurements. The last three lines are the calculated integral (Q_I), momentum transfer (Q_M), and viscosity (Q_V) cross sections in relative units. The values in parentheses are total errors for the integrated cross sections in the same relative units.

θ	10 eV	54.4 eV
0		
2	374 (105) E−0	
4	311 (87) E−0	237 (7) E+2
5	285 (80) E−0	174 (6) E+2
6	260 (73) E−0	129 (2) E+2
8	222 (62) E−0	772 (33) E+1
10	182 (59) E−0	445 (3) E+1
15		109 (1) E+1
20	952 (116) E−1	196 (3) E−0
30	278 (58) E−1	188 (8) E−1
40	106 (15) E−1	513 (23) E−2
50	705 (14) E−2	233 (26) E−2
60	351 (40) E−2	245 (1) E−2
70	146 (24) E−2	244 (2) E−2
80	629 (57) E−3	154 (46) E−2
90	100 (18) E−2	100 (6) E−2
100	119 (24) E−2	430 (88) E−3
110	129 (14) E−2	214 (11) E−3
120	102 (13) E−2	733 (273) E−3
130	649 (89) E−3	280 (34) E−2
140	348 (140) E−3	473 (84) E−2
148		790 (45) E−2
150	248 (25) E−3	
Q_I	118 (34) E−0	177 (35) E+1
Q_M	404 (114) E−1	123 (24) E−0
Q_V	601 (171) E−1	176 (34) E−0

elastic Q_I calculated from columns A and C gets better when the energy is raised from 20 eV to 54.4 eV but it is still not satisfactory (42%) at 54.4 eV. The ratios of inelastic Q_I with respect to the 3^2P one (columns B/A) at 54.4 eV show a systematic decrease. This tendency could not be attributed to our transmission as its variation is smaller than at lower energies. Also, this variation should be very small for the inelastic processes. Finally, we should point out that except for the elastic cross sections at 10 eV and 20 eV, our integral cross sections calculated from column C including the extrapolation procedure to zero and 180° are in excellent agreement with the integrated theoretical cross sections of Madison *et al* (1992). It means that applied extrapolation does not contribute significantly to the error. The difference between the two sets of integral elastic cross sections varies from 50% at 10 eV, 23% at 20 eV to only 6% at 54.4 eV. This difference is due to the extrapolated part of the $\sigma(\theta)$ curve (from zero to 15° at 10 eV). Although the values of Madison *et al* (1992) are lower than those calculated from column C they are still higher than those calculated from column A indicating, as already stated, the possibility of lower transmission for elastically scattered electrons in our experiment.

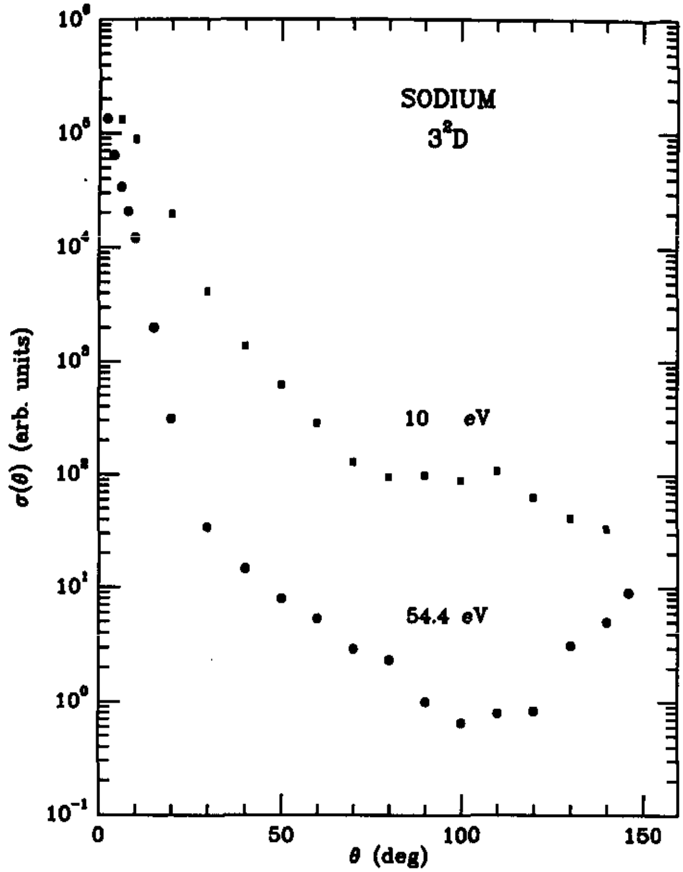

Figure 8. Relative differential cross sections of 3^2D at 10 and 54.4 eV.

4. Conclusion

The study presented in this paper is intended to produce the precise shape of $\sigma(\theta)$ for elastic scattering and excitation of sodium, a target used as a test case in many experiments. Although there have been a number of measurements and calculations done involving electron scattering by sodium at intermediate impact energies, some ambiguity still exists. Excitations of the higher states, 3^2D and 4^2P, were measured for the first time in this experiment, this was made possible with an apparatus energy resolution of 50 meV. States higher than these two were not resolved as separate peaks in the spectra and, therefore, not studied.

Results of absolute or relative $\sigma(\theta)$ as well as integrated cross sections are presented in tables 1-5 and figures 3, 5-9. Comparisons with existing theoretical and experimental results for the 3^2P state at 10 eV are given in figure 4. Detailed comparisons with the most recent calculations are given in the following paper by Madison *et al* (1992).

The present experiment acquires $\sigma(\theta)$ in a large range of scattering signals. The sodium resonant state is strongly coupled to all other states and, therefore, influences

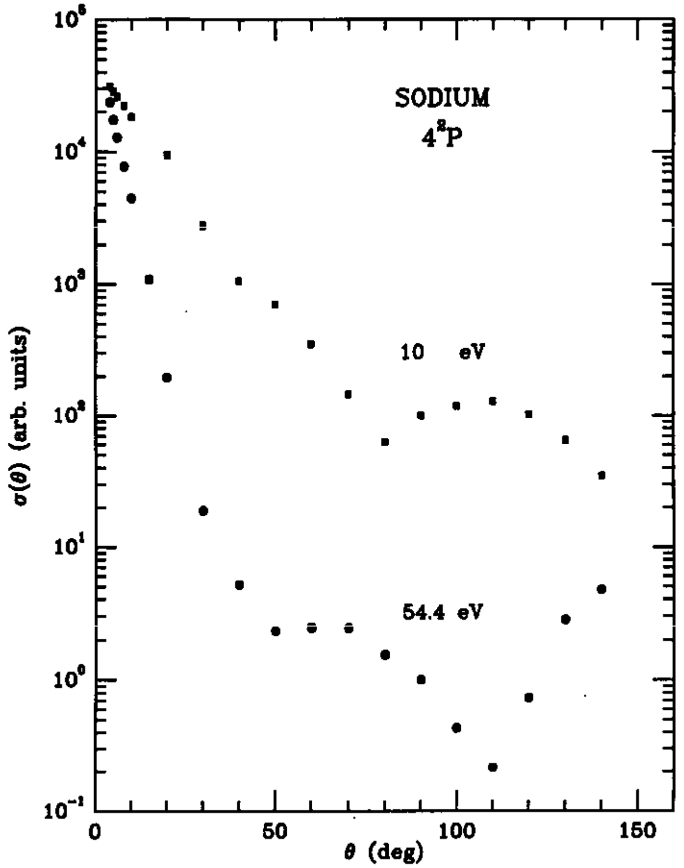

Figure 9. Relative differential cross sections of 4^2P at 10 and 54.4 eV.

Table 6. Intensity ratios for $\sigma(\theta)$ for elastic and inelastic transitions at 10° scattering angle (*, at 20°) with respect to the value of $\sigma(\theta)$ for the 3^2P state at the same angle. The values in parentheses are total errors in the intensity measurements.

Transition	10 eV	20 eV	54.4 eV
Elastic	897 (77) E−3*	254 (23) E−3	558 (56) E−3
4^2S	212 (27) E−4	350 (42) E−4	649 (83) E−4
3^2D	112 (9) E−3		208 (25) E−3
4^2P	709 (116) E−4*		112 (18) E−3

all excitation cross sections. This could be the reason why close coupling theories, treating exactly a limited number of states, overestimate the cross sections for elastic and the 3^2P state at larger scattering angles. It is a further challenge for theory to take into account all of these effects.

Table 7. Normalization factors for different normalization procedures: A, normalization to the optical oscillator strength; B, normalization to the integral cross sections from experiments by Phelps and Lin (1981); C, normalization to the theory obtained by equating the integrated experimental results to the equivalent integrated Madison *et al* (1992) DWB2PE values as described in the text. The $\sigma(\theta)$ obtained by multiplying values in tables 1-5 by these normalization factors are in units of 10^{-20} m^2 sr^{-1}, while the integrated cross sections are in units of 10^{-20} m^2.

Energy (eV)	Transition	A	B	C
10	Elastic	627E−4		406E−3
	3^2P	100E−2	121E−2	136E−2
	4^2S	870E−5	118E−4	288E−4
	3^2D	998E−5	115E−4	
	4^2P	396E−5	496E−5	676E−4
20	Elastic	106E−3		238E−4
	3^2P	100E−2	893E−3	976E−3
	4^2S	126E−4	943E−5	106E−4
54.4	Elastic	168E−4		239E−4
	3^2P	100E−2	106E−2	108E−2
	4^2S	139E−5	116E−5	957E−6
	3^2D	271E−6	203E−6	
	4^2P	400E−6	210E−6	972E−6

Acknowledgments

This work has been supported by the US–Yugoslav Joint Fund for Scientific and Technological Cooperation in cooperation with the NIST (JFP 598) and by RZN of SR Serbia, Yugoslavia. One of us (BM) thanks the JILA faculty and staff for their hospitality during his visit. One of us (LV) also acknowledges support by the NSF, PHY-9007571, during the preparation of this manuscript. We thank S Trajmar for a careful reading of the manuscript.

References

Allen L J, Brunger M J, McCarthy I E and Teubner P J O 1987 *J. Phys. B: At. Mol. Phys.* **20** 4861
Balashov V V, Grum-Grzhimailo A N and Klochkova O I 1989 *J. Phys. B: At. Mol. Opt. Phys.* **22** L669
Bransden B H and McDowell M R C 1978 *Phys. Rep.* **46** 249
Bray I, Konovolov D A and McCarthy I E 1991a *Phys. Rev.* A **44** 7179
—— 1991b *Phys. Rev.* A **44** 7830
Brinkmann R T and Trajmar S 1981 *J. Phys. E: Sci. Instrum.* **14** 245
Buckman S J and Teubner P J O 1979 *J. Phys. B: At. Mol. Phys.* **12** 1741
Carse G D 1972 *J. Phys. B: At. Mol. Phys.* **5** 1928
Filipović D, Pejčev V, Marinković B and Vušković L 1988 *Fizika* **20** 421
Gehenn and Reichert 1972 *Z. Phys.* **254** 28
Gien T T 1988 *J. Phys. B: At. Mol. Opt. Phys.* **21** 3767
Hertel I V and Rost K A 1971 *J. Phys. B: At. Mol. Phys.* **4** 690
Issa 1977 *PhD Thesis* Durham
Jiang T Y, Ying C H, Vušković L and Bederson B 1990 *Phys. Rev.* A **42** 3852
Kelley M H 1990 Private communication
Kennedy J V, Myerscough V P and McDowell M R C 1977 *J. Phys. B: At. Mol. Phys.* **10** 3759

Lorentz S R and Miller T M 1989 *Proc. 16th Int. Conf. on the Physics of Electronic and Atomic Collisions (New York)* ed A Dalgarno *et al* (Amsterdam: North-Holland) Abstracts p 198

Madison D H, Bartschat K and McEachran R P 1992 *J. Phys. B: At. Mol. Opt. Phys.* **25** 5199

Marinković B 1988 *PhD Thesis* University of Belgrade

Marinković B, Pejčev V, Filipović D, Čadež I and Vušković L 1988 *Proc. 14th Int. Symp. on the Physics of Ionized Gases (Sarajevo)* ed N Konjević *et al* (Sarajevo: Electrical Engineering Faculty) Contributed papers pp 25, 121

—— 1989 *Proc. 16th Int. Conf. on the Physics of Electronic and Atomic Collisions (New York)* ed A Dalgarno *et al* (Amsterdam: North-Holland) Abstracts p 133

Marinković B, Pejčev V, Filipović D and Vušković L 1991 *J. Phys. B: At. Mol. Opt. Phys.* **24** 1817

McCarthy I E, Mitroy J and Stelbovic A T 1985 *J. Phys. B: At. Mol. Phys.* **18** 2509

McClelland J J, Kelley M H and Celotta R J 1989 *Phys. Rev.* A **40** 2321

Mitroy J, McCarthy I E and Stelbovic A T 1987 *J. Phys. B: At. Mol. Phys.* **20** 4827 and private communication

Msezane A Z 1988 *Phys. Rev.* A **37** 1787

Msezane A Z, Handy C R, Mantica G and Lee J 1988 *Phys. Rev.* A **38** 1604 and private communication

Oza D H 1988 *Phys. Rev.* A **37** 2721

Phelps J O and Lin C C 1981 *Phys. Rev.* A **24** 1299

Shuttleworth T, Newell W R and Smith A C H 1977 *J. Phys. B: At. Mol. Phys.* **10** 1641

Srivastava S K and Vušković L 1980 *J. Phys. B: At. Mol. Phys.* **13** 2633

Teubner P J O, Buckman S J and Noble C J 1978 *J. Phys. B: At. Mol. Phys.* **11** 2345

Teubner P J O, Riley J L, Brunger M J and Buckman S J 1986 *J. Phys. B: At. Mol. Phys.* **19** 3313

Vušković L, Trajmar S and Register D F 1982 *J. Phys. B: At. Mol. Phys.* **15** 2517

Walters H R J 1973 *J. Phys. B: At. Mol. Phys.* **6** 1003

Wiese W L, Smith M W and Miles B M 1969 *Atomic Transition Probabilities, vol II Sodium Through Calcium* (NSRDS-NBS 22) (Washington, DC: US Govt Printing Office)